A MODEL OF THE GRAVITATIONAL FIELD OF AMALTHEA PART I: DERIVATION

KRZYSZTOF GOŹDZIEWSKI, ANDRZEJ J. MACIEJEWSKI
Institute of Astronomy, Nicolaus Copernicus University, Torún, Poland

and

PHILIP J. STOOKE
Department of Geography, University of Western Ontario, London, Ontario, Canada

(Received 11 February 1994)

Abstract. Utilizing the topographic model of Jovian moon Amalthea (Stooke, 1994) and supposing that its mass density is constant we derived its basic geometrical and dynamical characteristics. For calculations the harmonic model of topography of the degree and order 18 was selected. The model appears to fit the entire surface to a mean accuracy of a few hundred meters, except in the regions localized around longitudes 0° and 180°. On the basis of the harmonic expansion of the topography we estimated the volume ($V = 2.43 \pm 0.02\,\mathrm{km}^3$) and the mean radius of topography $r_0 = (79.7 \pm 0.2)$ km. Generalized moments of inertia up to the order 2, principal moments of inertia and orientation of the principal axes with respect to the original reference frame were also calculated. The results show that although Amalthea has extremely irregular shape it may be treated dynamically as an almost symmetric body ($B \simeq C$). Finally, the set of the Stokes coefficients up to the degree and order 9 was evaluated. The results are verified by direct numerical integration.

1. Introduction

Amalthea (JV) is a Jovian satellite which was observed by the Voyager 1 and Voyager 2 spacecraft. On the base of photographic images a detailed topographic model of Amalthea was derived by Stooke (1992). The topographic data are represented as a set of spherical cartographic coordinates of points lying on the satellite's surface. More precisely, the values of radii are given for equally spaced intervals ($5° \times 5°$) of longitude and latitude. In the cartographic coordinates the longitude is positive in the direction of clockwise rotation about the north pole and the latitude is measured from the plane of the equator.

In this work we use the planetocentric reference frame for the description of the shape of Amalthea as well for representation of its geometrical and dynamical characteristics.

According to the IAU convention of planetocentric coordinates the longitude is measured positive in *counter-clockwise* rotation about the north pole (thus positive east), the latitude is measured from the equator (positive north, negative south). The planetocentric reference frame is right-handed. The body-centered position vector $\mathbf{r}$ of a point $P(x, y, z)$ on the surface (see Figure 1) is given by

Earth, Moon, and Planets **64**: 243–264, 1994.

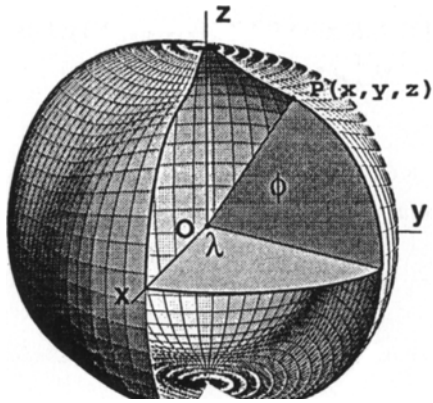

Fig. 1. Planetocentric reference frame.

$$\mathbf{r} = r(\phi, \lambda) \begin{pmatrix} \cos\phi \cos\lambda \\ \cos\phi \sin\lambda \\ \sin\phi \end{pmatrix} \tag{1}$$

where $r(\phi, \lambda)$ is the module of the radius vector $\mathbf{r}$.

The original data were transformed from the cartographic system to the planetocentric reference frame.

The shape of Amalthea is highly irregular. Its overall dimension was estimated as $270 \times 160 \times 150$ km. It was stated that the shape of Amalthea is too irregular to be approximated well by any ellipsoid (Veverka *et al.*, 1981; Stooke, 1992). The overall dimensions are given as maximum dimensions in three mutually orthogonal directions, not necessarily constrained to pass through a common point.

All the calculations we made on the base of an improved version of the topography model (Stooke, 1994). Using improved image processing techniques Stooke was able to indentify previously unseen topographic features in many of the Amalthea images. Comparisons of these topographic features with the latitude—longitude grid generated from the original model (Stooke, 1992) revealed parallax between the grid and the surface in one region. This has been eliminated in the revised model (Stooke, 1994), Further improvement may be possible in the region around longitude 330°, where the current model is based on a sneared image.

The STD errors of the topographic data can be only approximated. Uncertainties vary across the surface. The uncertainty of radius is about 5 km STD in the best areas, which are described in the revised system of coordinates as being between 70 degrees south and 90 degrees north, between longitudes 170° and 300° and again between longitudes 0° and 90°. Elsewhere the uncertainty is 2 or 3 times greater, worst of all at the south pole.

The lack of other reasonable models forced us to assume that the mass distribution in the interior of Amalthea is uniform. In all of the formulae presented in this paper we use this assumption although they could be written for a radial or more general distribution of the density.

2. Harmonic Expansion of the Topography

In the case of small, irregular celestial bodies (such as Amalthea) the approximation of a shape as a spheroid or ellipsoid (which is done for the big planets) is usually fairly unrealistic. For the modelling of dynamical properties of such bodies the detailed knowledge of their shapes is essential. For this purpose a discrete shape model is also unsatisfactory – one would like to have an analytic description of the figure in order to evaluate the dynamical characteristics, which are mostly represented by three dimensional integrals over the body's volume.

A favourable solution of the problem is to use a spherical expansion of the topography (Duxbury, 1989). Having a discrete description of the topography one can fit smooth harmonic models, varying easily the degree and order of the expansion. Under the assumption that the density has a radial or uniform distribution there exists an explicit relationship between topographic and gravity field harmonic coefficients. The topographic coefficients can be used to evaluate also other geometrical and dynamical characteristics of the body, e.g.: its volume, the mean radius, the equatorial radius, the mass, generalized moments of inertia, the tensor of inertia.

In the body-fixed, planetocentric reference frame the radius of the topography will be described as the expansion in terms of the real spherical harmonics (Bills and Ferrari, 1978):

$$r_t(\phi, \lambda) = \sum_{j=0}^{\infty} \sum_{m=0}^{m=j} \bar{P}_{jm}(\sin \phi)[\bar{a}_{jm} \cos(m\lambda) + \bar{b}_{jm} \sin(m\lambda)], \tag{2}$$

where (r_t, ϕ, λ) are spherical coordinates of a point of the body's surface. The set of coefficients $(\bar{a}_{jm}, \bar{b}_{jm})$ describes the shape completely.

The functions $\bar{P}_{jm}$ are normalized associated Legendre functions. The form of normalization we used is widely applied (see for example the article of Bills and Ferrari, 1978). The functions

$$P_j^m(x) = \frac{(1-x^2)^{m/2}}{2^j j!} \frac{d^{j+m}(x^2-1)^j}{dx^{j+m}}$$

are unnormalized associated Legendre functions of degree j and order m. The normalized functions are derived from the relation

$$\bar{P}_{jm}(x) = N_{jm} P_j^m(x),$$

with N_{jm} denoting the normalizing factor:

$$N_{jm} = \sqrt{(2 - \delta_{m0})(2j + 1)\frac{(j - m)!}{(n + m)!}}. \tag{3}$$

The normalized coefficients of the expansion (2) are related to unnormalized coefficients through the following formula

$$\bar{P}_{jm}\begin{matrix}\bar{a}_{jm}\\ \bar{b}_{jm}\end{matrix} = P_j^m \begin{matrix}a_{jm}\\ b_{jm}\end{matrix}.$$

Often it is more convenient to use the complex form of the expansion (2). It has the form (Martineč *et al.*, 1989)

$$r_t(\phi, \lambda) = \sum_{j=0}^{\infty} \sum_{m=j}^{m=-j} E_{jm} Y_{jm}(\phi, \lambda), \tag{4}$$

where now E_{jm} denote complex harmonic coefficients and $Y_{jm}(\phi, \lambda)$ are fully normalized complex spherical harmonics

$$Y_{jm}(\phi, \lambda) = P_{jm}(\sin \phi) e^{im\lambda}. \tag{5}$$

The functions $P_{jm}(\sin \phi)$ are fully normalized associated Legendre functions. The normalization is the same as widely used in quantum mechanics (Edmonds, 1960). If $P_j^m(x)$ denotes the unnormalized associated Legendre function and $\bar{P}_{jm}(x)$ its real fully normalized form, then the relation between them and P_{jm} can be written as

$$P_{jm}(x) = (-1)^m \sqrt{\frac{(2j + 1)(j - m)!}{4\pi(j + m)!}} P_j^m(x) \tag{6}$$

$$= (-1)^m \sqrt{\frac{1}{4\pi(2 - \delta_{m0})}} \bar{P}_{jm}(x). \tag{7}$$

The complex, fully normalized harmonic coefficients E_{jm} have then the form:

$$E_{jm} = (-1)^m \sqrt{\frac{4\pi(j + m)!}{(2j + 1)(j - m)!}} \frac{1}{(2 - \delta_{m0})} (a_{jm} - ib_{jm}) \tag{8}$$

$$= (-1)^m \sqrt{\frac{1}{4\pi(2 - \delta_{m0})}} (\bar{a}_{jm} - i\bar{b}_{jm}), \quad m \geqslant 0. \tag{9}$$

Here $\{a_{jm}, b_{jm}\}$ and $\{\bar{a}_{jm}, \bar{b}_{jm}\}$ denote real unnormalized and real fully normalized spectral harmonic coefficients, respectively. Because r_t is real, it follows that for $m \leqslant 0$:

$$Y_{j,-m} = (-1)^m Y^*_{jm}, \quad E_{j,-m} = (-1)^m E^*_{jm},$$

where the symbol * denotes the complex conjugation. Having the expansion (4), the k-th natural power can be computed recursively in the following way.

First let us compute the square of a radius r_t

$$r_t^2 = \sum_{j_1,m_1} \sum_{j_2,m_2} E_{j_1,m_1} E_{j_2,m_2} Y_{i_1,m_1} Y_{j_2,m_2} . \tag{10}$$

The spherical harmonics in the above formula have the same arguments, so their product can be expanded by means of Clebsch-Gordan coefficients (Landau and Lifshic, 1974)

$$Y_{j_1,m_1} Y_{j_2,m_2} = \sum_{j=|j_1-j_2|}^{j_1+j_2} \sum_{m=-j}^{j} \sqrt{\frac{(2j_1+1)(2j_2+1)}{4\pi(2j+1)}}\, C^{j0}_{j_1 0 j_2 0} C^{jm}_{j_1 m_1 j_2 m_2} Y_{jm} . \tag{11}$$

Inserting (11) into (10) and changing the order of summation:

$$r_t^2 = \sum_{j} \sum_{m=-j}^{m=j} E^{(2)}_{jm} Y_{jm} , \tag{12}$$

with the coefficients $E^{(2)}_{jm}$ computed as:

$$E^{(2)}_{jm} = \sum_{j_1,m_1} \sum_{j_2,m_2} \sqrt{\frac{(2j_1+1)(2j_2+1)}{4\pi(2j+1)}}\, C^{j0}_{j_1 0 j_2 0} C^{jm}_{j_1 m_1 j_2 m_2} E_{j_1,m_1} E_{j_2,m_2} . \tag{13}$$

Remark 1. The quadruple sum extends for infinite number of terms. In practice we have to use a finite number of coefficients of the topography radius expansion. The procedure for computation of the coefficients (13) consists of four loops over the indices j_1, j_2, m_1, m_2. To a coefficient $E^{(2)}_{jm}$ contribute only the terms which fulfil the condition $j_1 + j_2 \leq j \leq |j_1 - j_2|$ with $0 \leq j \leq j_{max}$. As was pointed out in the paper of Chao and Rubincam (1989), numerical computation of the sum (13) can be extremely tedious. For example, in the case of the topography model with $j_{max} = 18$, the sum describing one coefficient (13) contains about 1.3×10^5 coupling terms.

Remark 2. The formulae for numerical computation of the Clebsch-Gordan coefficients can be found in the book of Landau and Lifshic (1974) or in the article of Peč and Martineč (1989). For tests we used excellent procedures of the MATHEMATICA system (ThreeJSymbol and ClebshGordan).

Now, generalizing (12), the k-th power of the radius of topography can be written as

$$r_t^k = \sum_{j_1,m_1} \sum_{j_2,m_2} E^{(k-1)}_{j_1,m_1} E^{(1)}_{j_2,m_2} Y_{j_1,m_1} Y_{j_2,m_2} \equiv \sum_{j} \sum_{m} E^{(k)}_{jm} Y_{jm} , \quad k > 1, \tag{14}$$

where $E_{jm}^{(k-1)}$ are expansion coefficients of the $(k-1)$ power of r_t, $E_{jm}^{(1)} \equiv E_{jm}$. The general form of the coefficients is the same as (13):

$$E_{jm}^{(k)} = \sum_{j_1,m_1} \sum_{j_2,m_2} \sqrt{\frac{(2j_1+1)(2j_2+1)}{4\pi(2j+1)}}\, C_{j_1 0 j_2}^{j0} C_{j_1 m_1 j_2 m_2}^{jm} E_{j_1,m_1}^{(k-1)} E_{j_2,m_2}^{(1)} \tag{15}$$

3. Numerical Integration

If one knows the shape of a body and its internal density distribution then the direct method of numerical integration can be used for evaluation of its gravitational and dynamical characteristics (Sagitov *et al.*, 1981; Chao and Rubincam, 1989). Most of them can be described as integrals over the body's volume. In the spherical coordinates system such a characteristic can be described as

$$I = \int_{\Omega(\phi,\lambda)} \int_{r=0}^{r=r(\phi,\lambda)} r^n(\phi,\lambda)\rho(r,\phi,\lambda) f(\phi,\lambda)\, \mathrm{d}r\, \mathrm{d}\Omega, \tag{16}$$

where (r, ϕ, λ) denote a point in the body, ρ is the density at this point and f is a function of angular variables only. For example, the moments of inertia and the Stoke's coefficients of the harmonic expansion of the gravitational potential have the form of (16).

Now let us assume that the density of the body is constant (we put $\rho = \rho_c = const$). Then the three-dimensional integral (16) can be reduced to a two-dimensional one. Performing the integration over r we obtain

$$I = \rho_c \frac{1}{n+1} \int_{\Omega(\phi,\lambda)} r^{n+1}(\phi,\lambda) f(\phi,\lambda)\, \mathrm{d}\Omega. \tag{17}$$

For numerical calculation of this integral we choose, after some tests, the 10-points Gauss-Legendre quadrature as a kernel of the integration procedure.

The idea we applied is as follows. The problem of two-dimensional integration is easily reduced to evaluation of one-dimensional integrals. We divide successively the interval of integration and apply for any of its part the Gauss-Legendre quadrature. Finally, the value of a one-dimensional integral is computed with the help of polynomial extrapolation constructed on a base of, say n divisions of the initial interval of integration. If the relative results of the n-th and $(n-1)$-th approximations differ less than a predetermined accuracy ϵ, the procedure is stopped. In practice we observed that the maximal number of divisions n was of order 30. The value of ϵ was of the order $1.0e-5$.

The procedure of evaluating the two-dimensional integrals is adopted from Press *et al.* (1992).

4. The Moments of Inertia

The moments or product of inertia affect rotational and orbital motion of planetary bodies. Thus knowledge of them is essential in studies of motions.

Let us introduce the generalized moments of inertia. The integral of inertia (generalized product of inertia) of order (i, j, k) with respect to a body-fixed reference frame is defined as (Paul, 1974)

$$M_{ijk} = \int_V x^i y^j z^k \, \mathrm{d}M, \tag{18}$$

where (x, y, z) are Cartesian coordinates. It was shown (Duboshin, 1974) that the gravitational potential of a body can be represented in terms of the integrals (18). In the paper of Paul (1974) a similar representation for the mutual potential between two graviting bodies of finite sizes is constructed. The result is worth mentioning because an alternative representation of the mutual potential in terms of spherical functions (Šlidlichovský, 1978) is very complicated and difficult to use in applications.

Computations of the generalized moments of inertia can be straightforward (by numerical integration) if the mass distribution as well as the geometrical shape of a body is known. In the case of Amalthea we use the approximation of uniform density, thus the integrals (18) can be described in general in the form of (17).

On the basis of the generalized moments of inertia one can compute the principal axes and the principal moments of inertia of the body. In matrix form the moment of inertia of a body model with density distribution $\rho(\mathbf{r})$ is given by:

$$\mathbf{I} = \int_V \rho(\mathbf{r}) \begin{pmatrix} y^2 + z^2 & -xy & -xz \\ -xy & z^2 + x^2 & -yz \\ -xz & -yz & x^2 + y^2 \end{pmatrix} \mathrm{d}V. \tag{19}$$

In terms of the generalized moments of inertia the inertia tensor (19) reads

$$\mathbf{I} = \begin{pmatrix} M_{020} + M_{002} & -M_{110} & -M_{101} \\ -M_{110} & M_{200} + M_{002} & -M_{011} \\ -M_{101} & -M_{011} & M_{200} + M_{002} \end{pmatrix}. \tag{20}$$

The orientation of principal axes and the inertia moments associated with them can be obtained by solving the eigen-problem for the matrix (20).

4.1. The moments of inertia versus topography

On the basis of the harmonic expansion (4) the generalized moments of inertia can be expressed analytically.

The moment of the order (0, 0, 0) describes the mass of a body

$$M \equiv M_{000} = \int_\Omega \int_{r=0}^{r=r_t(\phi,\lambda)} \rho(\mathbf{r}) r^2 \cos\phi \, \mathrm{d}\phi \, \mathrm{d}\lambda \, \mathrm{d}r$$

Assuming the constant density $\rho(\mathbf{r}) = \rho_c$, inserting the expansion (4) of r_t into the above formula and integrating over the full solid angle we obtain:

$$M = \rho_c \frac{2}{3}\sqrt{\pi}\, E_{00}^{(3)} \equiv \rho_c V, \quad \text{thus } V = \frac{2}{3}\sqrt{\pi}\, E_{00}^{(3)}, \tag{21}$$

where V denotes the volume of the body.

The moments of the first order measure the offsets of the center of mass of the body from the origin of the coordinates system. With the assumptions as above, the analytical integration gives

$$\begin{aligned} M_{100} &= -\rho_c \sqrt{\frac{\pi}{6}}\, \Re E_{11}^{(4)}, \\ M_{010} &= \rho_c \sqrt{\frac{\pi}{6}}\, \Im E_{11}^{(4)}, \\ M_{001} &= \rho_c \frac{1}{2\sqrt{3}}\sqrt{\pi}\, E_{10}^{(4)}. \end{aligned} \tag{22}$$

Dividing the moments by the expression for the mass (21) one gets the offsets:

$$\bar{x} = -\frac{1}{2}\sqrt{\frac{3}{2}}\frac{\Re E_{11}^{(4)}}{E_{00}^{(3)}}, \quad \bar{y} = \frac{1}{2}\sqrt{\frac{3}{2}}\frac{\Im E_{11}^{(4)}}{E_{00}^{(3)}}, \quad \bar{z} = \frac{\sqrt{3}}{4}\frac{E_{10}^{(4)}}{E_{00}^{(3)}}. \tag{23}$$

For computing the inertia tensor it is enough to evaluate the generalized moments of inertia of the second order as in (20)

$$\begin{aligned} M_{200} &= \rho_c \frac{2}{5}\sqrt{\pi}\left(\frac{1}{3}E_{00}^{(5)} - \frac{1}{3\sqrt{5}}E_{20}^{(5)} + \sqrt{\frac{2}{15}}\,\Re E_{22}^{(5)}\right), \\ M_{020} &= \rho_c \frac{2}{5}\sqrt{\pi}\left(\frac{1}{3}E_{00}^{(5)} - \frac{1}{3\sqrt{5}}E_{20}^{(5)} - \sqrt{\frac{2}{15}}\,\Re E_{22}^{(5)}\right), \\ M_{002} &= \rho_c \frac{2}{5}\sqrt{\pi}\left(\frac{1}{3}E_{00}^{(5)} + \frac{2}{3\sqrt{5}}E_{20}^{(5)}\right), \\ M_{110} &= -\rho_c \frac{2}{5}\sqrt{\frac{2}{15}}\sqrt{\pi}\,\Im E_{22}^{(5)}, \\ M_{101} &= -\rho_c \frac{2}{5}\sqrt{\frac{2}{15}}\sqrt{\pi}\,\Re E_{21}^{(5)}, \end{aligned} \tag{24}$$

$$M_{011} = \rho_c \frac{2}{5}\sqrt{\frac{2}{15}}\sqrt{\pi}\,\mathfrak{T}E_{21}^{(5)}.$$

Thus the inertia tensor reads:

$$I_{11}/M = \frac{2}{5}\left(E_{00}^{(5)} + \frac{1}{\sqrt{5}}E_{20}^{(5)} - \sqrt{\frac{3}{10}}\,\mathfrak{R}E_{22}^{(5)}\right)/E_{00}^{(3)}$$

$$I_{22}/M = \frac{2}{5}\left(E_{00}^{(5)} + \frac{1}{\sqrt{5}}E_{20}^{(5)} + \sqrt{\frac{3}{10}}\,\mathfrak{R}E_{22}^{(5)}\right)/E_{00}^{(3)}$$

$$I_{33}/M = \frac{2}{5}\left(E_{00}^{(5)} - \frac{1}{2\sqrt{5}}E_{20}^{(5)}\right)/E_{00}^{(3)}$$

$$I_{12}/M = -\frac{2}{5}\sqrt{\frac{3}{10}}\,\mathfrak{T}E_{22}^{(5)}/E_{00}^{(3)}, \tag{25}$$

$$I_{13}/M = -\frac{2}{5}\sqrt{\frac{3}{10}}\,\mathfrak{R}E_{21}^{(5)}/E_{00}^{(3)},$$

$$I_{23}/M = \frac{2}{5}\sqrt{\frac{3}{10}}\,\mathfrak{T}E_{21}^{(5)}/E_{00}^{(3)}.$$

Remark 3. The terms I_{11}, I_{22}, I_{22} are *not* principal moments of inertia as is suggested by the paper of Martineč *et al.* The off-diagonal elements, given by (25), do not vanish unless the appropriate topography coefficients have non-zero values. Generally, the original reference frame does not coincide with the frame of principal axes.

Remark 5. The integrals describing the generalized moments of inertia can also be computed easily in the cases when the density distribution is radial (not necessarily uniform). The problem is reduced to evaluation of integrals which have the following form:

$$I_{qsjm} = \int_{-1}^{1} x^q (1-x)^s P_j^m(x)\,\mathrm{d}x, \quad q \geqslant 0, \quad 2s = k, \quad k \text{ is integer.}$$

This can be done by application of the idea described in the book of Antonov (Antonov *et al.*, 1988). The integrals can be computed recurrently, on the base of recurrent relations for the associated Legendre functions.

5. Stokes Gravity Coefficients

In a body-fixed, right-handed Cartesian coordinate system the external gravitational field U at a point (r, ϕ, λ) is given by the standard formula

$$U(r, \phi, \lambda) = \frac{GM}{r} \sum_{j=0}^{\infty} \left(\frac{r_0}{r}\right)^j \sum_{m=0}^{l} \bar{P}_{jm}(\sin\phi)(\bar{C}_{jm} \cos m\lambda + \bar{S}_{jm} \sin m\lambda), \tag{26}$$

where G denotes the gravitational constant, M is the mass of the body, r_0 denotes a reference radius. The dimensionless coefficients of the expansion are taken here in the real, normalized form.

In a general form the coefficients are given by integrals (Chao and Rubincam, 1989)

$$\begin{matrix} \bar{C}_{jm} \\ \bar{S}_{jm} \end{matrix} = \frac{1}{(2j+1)Mr_0^j} \int_V \rho(r, \phi, \lambda)\, r^j\, \bar{P}_{jm}(\sin\phi) \begin{matrix} \cos m\lambda \\ \sin m\lambda \end{matrix} \mathrm{d}V, \tag{27}$$

where the integration is performed over the volume V of the body. If the density $\rho = \rho_c \equiv const$ then the coefficients depend on the topography only. In this case the formula (27) has the same form as the integral (17) and explicitly

$$\begin{matrix} \bar{C}_{jm} \\ \bar{S}_{jm} \end{matrix} = \frac{1}{(2j+1)(j+3)Vr_0^j} \int_{(\Omega)} r^{(j+3)}(\Omega)(\, \bar{P}_{jm}(\sin\phi) \begin{matrix} \cos m\lambda \\ \sin m\lambda \end{matrix} \mathrm{d}\Omega. \tag{28}$$

On the basis of this surface integral the Stokes' coefficients can be computed by numerical integration.

Under the same assumptions the Stokes coefficients can be expressed analytically by the harmonic coefficients (15). The external potential (26) written in the complex form (Martineč *et al.*, 1989) is:

$$U(r, \Omega) = \frac{GM}{r} \sum_{j=0}^{\infty} \left(\frac{r_0}{r}\right)^j \sum_{m=-j}^{m=j} A_{jm} Y_{jm}(\Omega), \tag{29}$$

where the coefficients of expansion are complex and fully normalized in the complex sense. They are expressed by the integrals over the volume of the body:

$$A_{jm} = \frac{4\pi}{(2j+1)Mr_0^j} \int_{(\Omega)} \int_{r=0}^{r=r_t(\Omega)} r^{(j+2)}(\Omega)\, \rho(r, \Omega)\, Y^*(\Omega)\, \mathrm{d}r\, \mathrm{d}\Omega. \tag{30}$$

If the body is homogeneous then the three-dimensional integral (30), after performing integration over r is reduced to surface integral. Now we can replace a power of r_t by its complex expansion (14). Finally, using the formula for the volume (21) one gets:

$$A_{jm} = \frac{6\sqrt{\pi}}{(j+3)(2j+1)} \frac{E_{jm}^{(j+3)}}{E_{00}^{(3)}} \tag{31}$$

This represents the relationship between the gravity and the topography. The formula is exact. A discussion of applications of this formula can be found in papers of Chao and Rubincam (1989) and Martinec *et al.* (1989). It should be noted that in the case of highly irregular bodies one should not utilize the first order approximation of (31), as it was done in the paper of Duxbury (1989). Such an approach gives unrealistic results.

6. Numerical Results

6.1. Harmonic expansion of the topography

For the expansion of the normalized coefficients of the topography we applied the straightforward method of least squares. The model is defined by the expansion (2) truncated on some value $j = j_{max}$. It is linear with respect to the unknown coefficients. This allows to use the linear method of least squares. For computations we adopted the procedure LFIT taken from the book of Press *et al.* (1992).

The problem of a proper choice of the value $j_{\max}$ arises here. As a test indicating goodness of the fit one could use the behaviour of the reduced χ^2 (Bevington, 1969), computed for a number of models with increasing degree $j_{\max}$. As shown in Figure 2, the choice of $j_{\max}$ is formally almost obvious—the higher order the model is, the better the fit seems to be. However, because of the final goal – computation of the Stokes gravity coefficients and the generalized moments of inertia on the base of the expansions – the model of shape should be of as small degree and order as possible. This conclusion could be argued from Remark 1 of Section (2).

Finally, as a compromise forced by the problem remarked before, we used the model with $j_{\max} = 18$. The choice is based on numerical observation of the behaviour of characteristics, which can be derived from the topography expansion and their dependence on the maximal degree of a model. The results are presented on Figures 3–6.

The Figures 3 and 4 shows changes of the volume of Amalthea and the mean radius r_0 defined here as $\bar{a}_{00}$. The variations of the volume for $j_{\max} > 18$ are almost negligible, they are of order 0.1%. The next test is shown on Figures 5 and 6. They show numerical values of the Stokes coefficients (we choose some low degree coefficients) as functions of the maximal degree of the topographic expansion. They demonstrate that the choice of the model of degree 18 is at least safe. The relative changes of the coefficients are of the order 0.1%.

In the next test we computed the mean and maximal difference in radius vector as calculated from the harmonic models and by linear interpolation of the original data. This is presented in Figures 7–8. For calculations we used the grid with resolution 1° in both of the angular coordinates. Again, the mean differences are comparable, starting from the models with $j_{\max} \geq 18$.

For all the models tested, the longitude on which the maximal difference appears

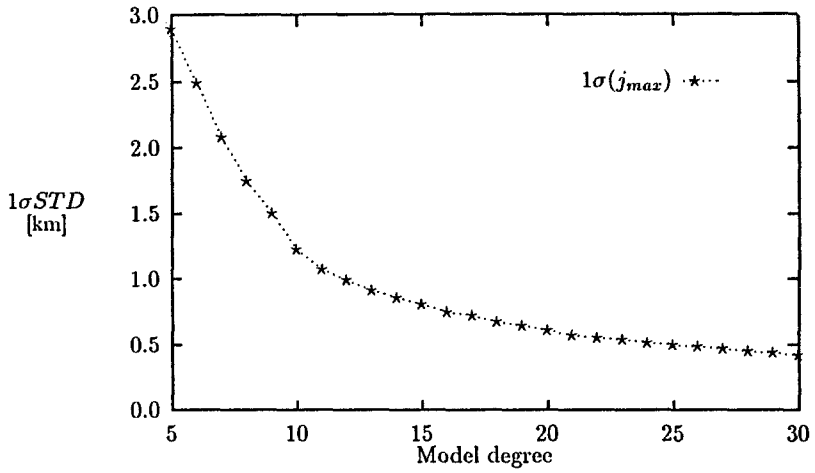

Fig. 2. Postfit STD errors of the linear least squares fit as a function of the maximal degree of harmonic expansion of the topography radius.

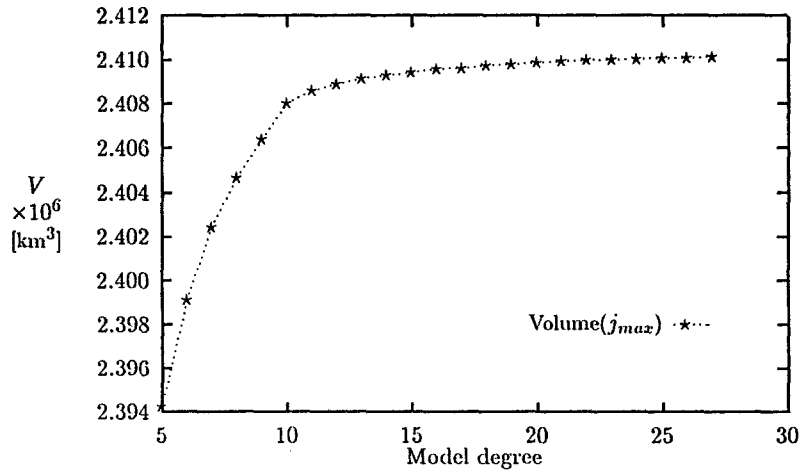

Fig. 3. Variations of the numerical estimation of the volume of Amalthea, as derived from harmonic expansions of the radius of topography.

is localized around 180°. An example of a global map of the differences for the model of the degree 18 is shown on Figure 9. It is surprising that maximal differences are much more bigger (of the order of one magnitude) than the mean values. For $j_{\max} \geqslant 18$ they stabilize on the value of about 3–4 km (see Figure 7).

The harmonic model of degree and order 18 was compared with the original data. Figure 10 shows 3D views of the shape described by the harmonic model from six mutually perpendicular directions. Note, that the planetocentric reference

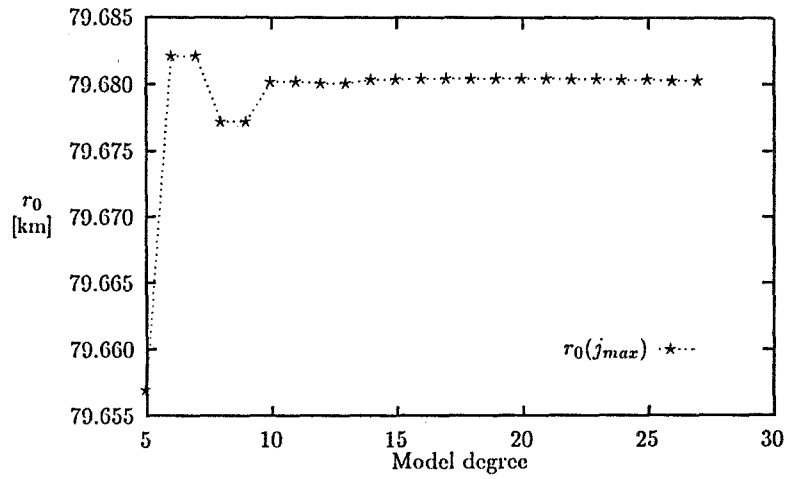

Fig. 4. Changes in the mean radius of Amalthea, computed from topography expansion models.

frame is used. The views may be compared with analogous figures (based on the earlier shape model) in the paper of Stooke (1992). The coincidence of our model with the original data is apparently very good. This may be expressed in numbers: 1σ STD calculated for all of the control points, describing the shape of Amalthea, is of the order 0.6 km.

6.2. Geometric characteristics of Amalthea

The mean radius r_0 of the topography of Amalthea determined on the basis of the harmonic model $j_{\max} = 18$ is $r_0 = 79.7 \pm 0.2$ km.

The mean equatorial radius is defined as (Martineč *et al.*, 1989)

$$a_e = \frac{1}{2\pi}\int_0^{2\pi} r_t(0, \lambda)\, \mathrm{d}\lambda$$

and may by expressed in terms of the topography expansion:

$$a_e = r_0\left[1 + \sum_{j=1}^{\infty} (-1)^j \sqrt{\frac{4j+1}{4\pi}}\frac{(2j-1)!!}{(2j)!!}\right].$$

This leads to numerical value $a_e \simeq 79.86$ km.

The volume of Amalthea was computed by numerical integration and by application of the formula (21). The volume was estimated earlier by Veverka (1981): $2.4 \pm 0.5 \times 10^6$ km^3 and Stooke (1992): $2.5 \pm 0.5 \times 10^6$ km^3. Our estimate is very similar. Numerical integration gave

$$V = 2.44 \pm 0.02 \times 10^6 \text{ km}^3.$$

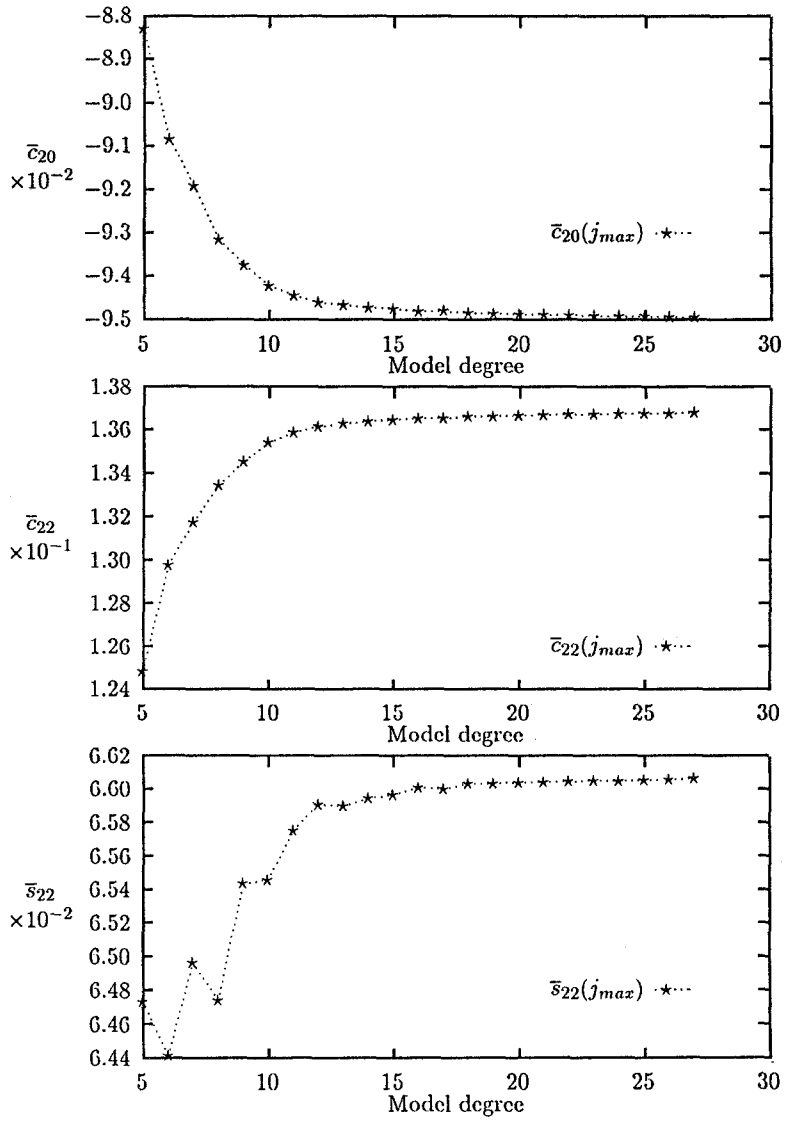

Fig. 5. Changes in the normalized Stokes coefficients computed from topography expansion models.

It can be compared with the estimate derived from the harmonic expansion with $j_{\max} = 18 - V = 2.41 \times 10^6$ km^3 (relative difference is 0.25%). Because the errors of the shape model are in fact not uniform and not well localized we tried to estimate the error of the volume as follows. To the original data was added a random noise of uniform distribution and the numerical integration was performed on the basis of a number of such noised shape models. The final value of a integral was next evaluated as the mean. The errors of the topography radius were sampled from the interval (−15, +15) km, the number of noised models was 100. The

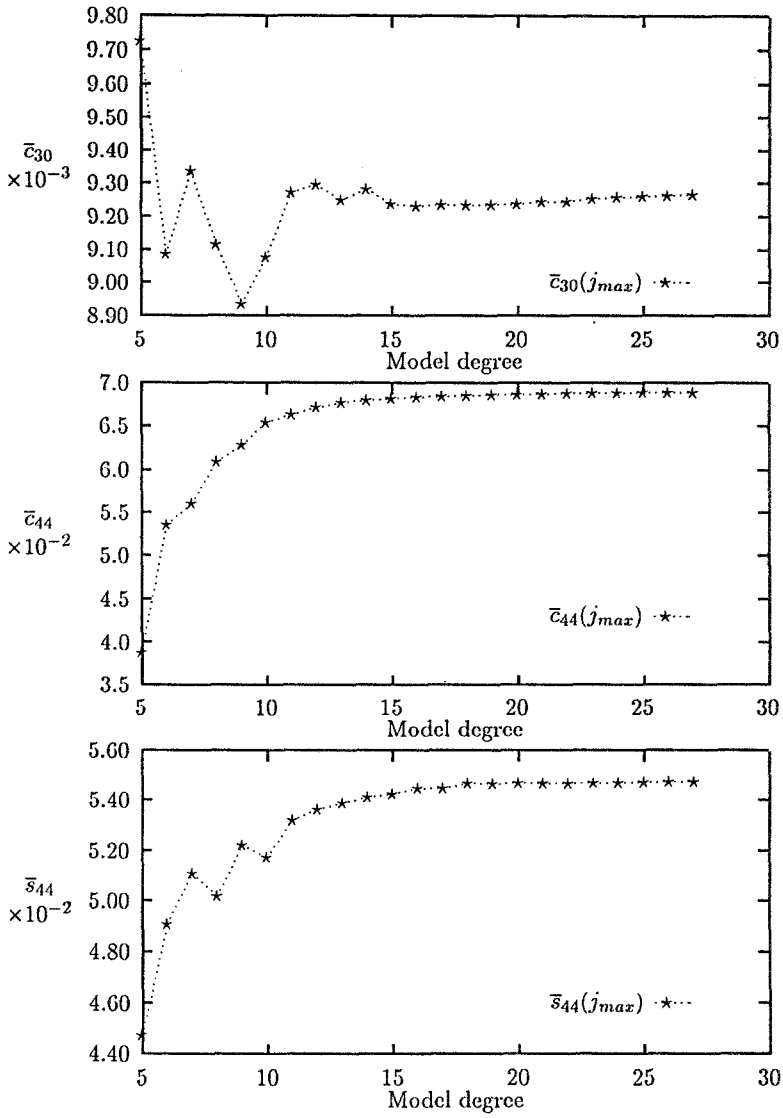

Fig. 6. Changes in the normalized Stokes coefficients computed from topography expansion models (*continued*).

same method was applied for the estimation of errors of the generalized moments of inertia.

6.3. The moments of inertia

The computation of the generalized moments of inertia was performed by means of numerical integration (as described in the Section 3) and the results were

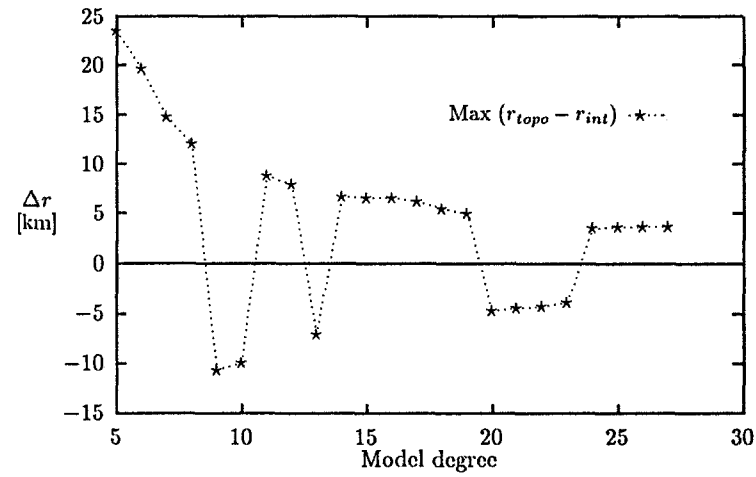

Fig. 7. Maximal differences in radius of topography as derived from harmonic expansions of (r_{topo}) and computed by linear interpolation of the original shape model (r_{int}).

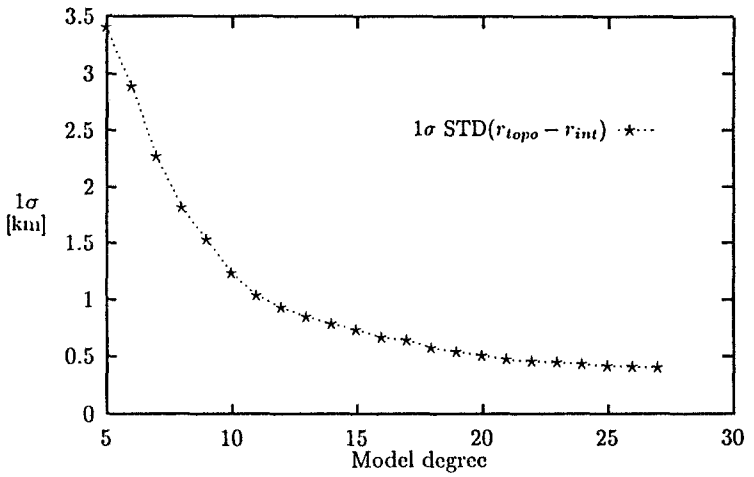

Fig. 8. Mean differences in radius as derived from harmonic expansions of the topography (r_{topo}) and computed by linear interpolation of the original shape model (r_{int}). The grid of $1^0 \times 1^0$ is used for the angular coordinates (ϕ, λ).

compared with the values obtained on the basis of the harmonic model of topography of the degree and order 18. The results are presented in Table I.

Differences between numerical and topographical estimations are in the range of few percent. Moments of the first order which express the shift of the center-of-figure of Amalthea from the center of the original reference frame are less than

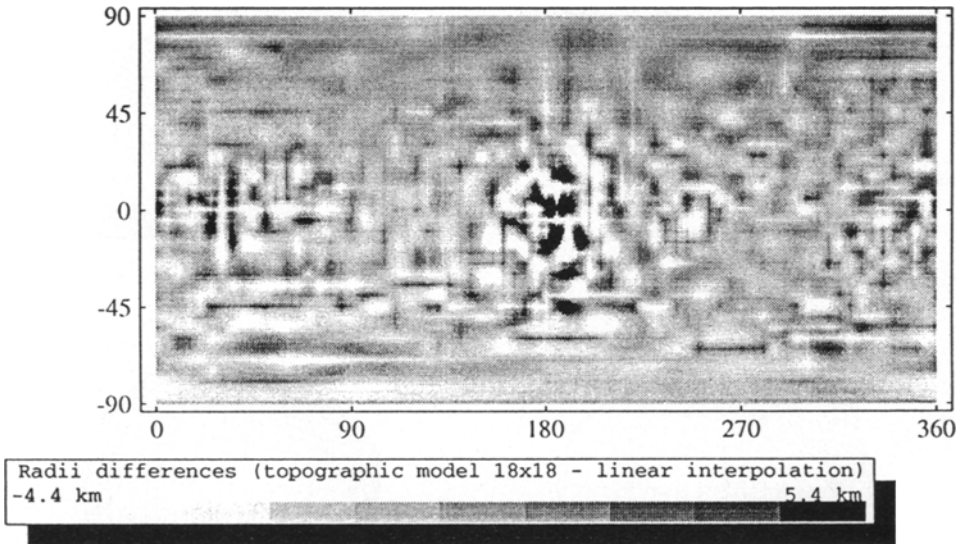

Fig. 9. Differences in radii as computed by linear interpolation on the basis of the original Amalthea's shape model of Stooke (1994) and derived from harmonic expansion of the degree and order 18. A grid 1° by 1° in both of the angular variables was applied (the planetocentric reference frame was used). The maximal differences are localized around longitudes close to 180°.

1 km. Thus, in practice they can be neglected. This result agrees with the conclusion of Stooke (1992).

Knowing the inertia tensor we are able to determine the orientation of the principal axes of Amalthea and the principal moments of inertia. The orientation will be described by the Euler angles of the type 3–2–1. The angles describe subsequent rotations of the body-fixed coordinate axes into the direction of the principal axes of inertia. They are determined in the process of diagonalization of the inertia tensor. Table II shows results which are derived when using the inertia tensor estimated by numerical integration. The xy planes of the principal and original frames are almost coinciding. The x principal axis is displaced from the point ($\phi = 0°$, $\lambda = 0°$) by about 16°. The values of principal moments of inertia shows that the moon is almost dynamically symmetric.

6.4. Stokes gravity coefficients

The coefficients of harmonic expansion of the external gravitational potential of Amalthea we determined in three independent ways

A numerical integration using the original data points (linear interpolation of radii in spherical coordinates was applied),

B numerical integration over the shape described by the harmonic model of the degree and order 18,

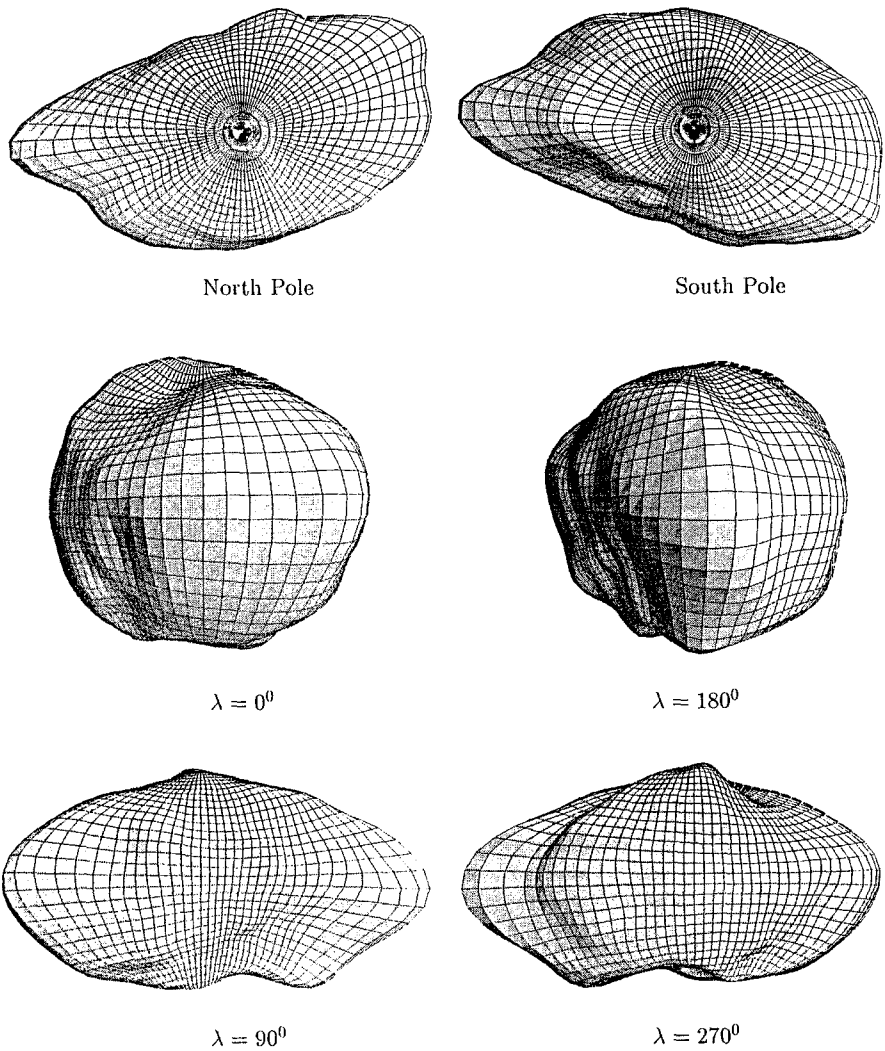

Fig. 10. Views of the body of Amalthea from six mutually perpendicular directions, computed on the base of harmonic expansion of the topography (a model of the degree and order 18 was used). From the top: north and south pole views, equatorial projections for $\lambda = 0°$, 180°, 90° and 270°.

C analytically, on the basis of the formula 31 with $j_{\max} = 18$.

The method **B** was applied in order to check the internal consistency of the numerical method of integration we used. A comparision of the results obtained by the three methods is given in Table III. Differences between results derived from methods **A** and **C** are very small. Their presence may be explained by the fact that although the analytical formula (31) is exact, during evaluation of subsequent

TABLE I

Generalized moments of inertia. The first order moments are normalized by the factor Mr_0, the moments of the second order by the factor Mr_0^2.

Order	Numerical integration	1σ	From Topography	Difference (%)
M_{100}	−0.009	0.008	−0.011	8.0
M_{010}	−0.006	0.004	−0.006	2.5
M_{001}	−0.008	0.003	−0.008	3.4
M_{110}	0.085	0.003	0.093	9.7
M_{101}	0.002	0.003	0.002	3.7
M_{011}	0.006	0.002	0.006	3.5
M_{200}	0.527	0.008	0.524	0.6
M_{020}	0.177	0.002	0.171	3.2
M_{002}	0.141	0.001	0.136	3.9
	Diagonal elements of the inertia tensor			
I_{xx}	0.318	0.003	0.307	3.5
I_{yy}	0.668	0.008	0.659	1.3
I_{zz}	0.704	0.008	0.695	1.2

TABLE II

Inertial characteristics of Amalthea computed using the expansion of topography and numerical integration (values in brackets).

Principal moments of inertia (in terms of Mr_0^2)		
A	B	C
0.292 (0.283)	0.686 (0.668)	0.705 (0.697)
Orientation of principal axes (3–2–1 Euler angles)		
ϕ	θ	ψ
13.0° (14.0°)	−0.5° (−0.5°)	16.5° (19.3°)

expansions (15) the sums had to be catted on the same number of terms. A comparison of the results given by the methods **A** and **C** shows however that distinctions between them have systematic trends. In order to explain their presence we made a careful inspection of the behaviour of appropriate integrands. This showed that some of them strongly depend on displacements in r_t, especially in the areas close to the equator. Thus we could state that even small differences between radii, calculated by linear interpolation and by application of a nonlinear model of the shape, may cause big changes in the values of appropriate integrals. In our case the differences in radii are of the order of a few percent in small areas (see Figure 9). However it has dramatic consequences – this effect changes the numerical values of Stokes coefficients up to 50%. Thus we may conclude that in order to estimate values of Stokes coefficients it is better to describe the shape by harmonic or other nonlinear model than interpolating linearly the original data.

Table IV presents three sets of real, fully normalized Stokes coefficients up to

TABLE III

Real, fully normalized Stokes coefficients of the external gravitational field of Amalthea. Differences [%] in results derived from numerical integration on the base of the original shape model (A), by numerical integration of the harmonic model 18 × 18 (B) and by analytical formulae, using also the harmonic model 18 × 18 (C).

		Method A-C		Method B-C				Method A-C		Method B-C	
j	m	δ_C	δ_S	δ_C	δ_S	j	m	δ_C	δ_S	δ_C	δ_S
1	0	3.70	−0.00	−0.01	−0.00	7	0	−7.30	−0.00	0.26	−0.00
1	1	8.87	−1.38	−0.06	0.02	7	1	−11.92	−2.91	1.15	−0.36
2	0	1.21	−0.00	−0.01	−0.00	7	2	7.10	−7.40	−0.28	9.82
2	1	−9.44	−0.96	0.05	0.02	7	3	9.46	8.20	−0.98	−0.20
2	2	−1.40	−0.99	0.01	0.01	7	4	−7.35	−2.29	0.28	−0.71
3	0	−1.22	−0.00	0.02	−0.00	7	5	−7.63	−29.61	0.87	2.46
3	1	−9.63	1.56	0.23	−0.04	7	6	8.27	3.26	−0.12	0.25
3	2	1.57	0.28	−0.02	−0.01	7	7	6.55	9.60	−0.78	−1.26
3	3	4.04	−0.39	−0.09	0.01	8	0	−7.93	−0.00	0.88	−0.00
4	0	−3.17	−0.00	0.06	−0.00	8	1	8.48	9.85	−0.72	1.45
4	1	4.15	0.92	−0.03	−0.02	8	2	8.06	7.97	−0.98	−0.47
4	2	3.19	2.63	−0.07	−0.02	8	3	−8.99	−9.08	0.61	−2.10
4	3	−4.19	−0.94	0.09	−0.03	8	4	−8.41	−8.43	1.28	0.68
4	4	−3.50	−2.67	0.11	−0.05	8	5	10.56	5.79	−0.31	2.20
5	0	3.96	−0.00	−0.03	−0.00	8	6	8.57	9.03	−1.68	−1.20
5	1	11.96	−0.61	−0.54	0.18	8	7	−12.54	−2.86	−0.19	−1.59
5	2	−3.95	1.79	0.04	−0.26	8	8	−8.02	−8.88	1.66	1.92
5	3	−7.00	−1.54	0.35	−0.04	9	0	6.68	−0.00	−1.51	−0.00
5	4	4.15	0.78	−0.06	0.01	9	1	13.68	12.57	−2.68	−0.41
5	5	5.26	43.86	−0.27	−1.96	9	2	−7.03	−16.56	1.46	−15.15
6	0	5.59	−0.00	−0.26	−0.00	9	3	−11.35	−37.39	2.48	7.25
6	1	−7.32	−3.62	0.11	−0.41	9	4	7.94	8.86	−1.39	2.68
6	2	−5.68	−5.28	0.30	0.11	9	5	9.33	28.68	−2.32	−4.22
6	3	7.64	2.51	−0.10	0.55	9	6	−9.89	−7.38	1.13	−0.82
6	4	5.99	5.27	−0.42	−0.21	9	7	−8.14	−13.00	2.21	2.96
6	5	−7.62	−0.46	−0.09	−0.30	9	8	14.29	6.31	−0.71	0.36
6	6	−6.24	−5.31	0.57	0.42	9	9	7.32	9.30	−2.18	−2.76

the degree and order 9. The first two sets are evaluated by application of the methods A and C. We present also mean values of the coefficients (labeled by D) and their STD errors as estimated by the same approach as in the case of the generalized moments of inertia. However, because the calculations of Stokes coefficients are numerically much more expensive, the errors are determined on the basis of 10 noised models of the shape. The first degree harmonics represent a displacement of the center-of-figure of the model from the center of the original reference frame:

$$\bar{x}_t = r_0\sqrt{3C_{11}} \simeq -1.05\ \text{km}\ (-0.75\ \text{km})$$

$$\bar{y}_t = r_0\sqrt{3S_{11}} \simeq -0.42\ \text{km}\ (-0.50\ \text{km})$$

$$\bar{z}_t = r_0\sqrt{3C_{10}} \simeq -0.52\ \text{km}\ (-0.62\ \text{km})$$

TABLE IV

Real fully normalized Stokes coefficients of the external gravitational field of Amalthea (in terms of 10^{-2}). Reference radius is $r_0 = 79.68$ km. Meaning of the indices A, B, D is explained in the text.

j	m	$\bar{C}^{A}_{jm}$	$\bar{S}^{A}_{jm}$	$\bar{C}^{B}_{jm}$	$\bar{S}^{B}_{jm}$	$\bar{C}^{D}_{jm}$	σ_C	$\bar{S}^{D}_{jm}$	σ_S
1	0	−0.461		−0.445		−0.378	0.147		
1	1	−0.636	−0.325	−0.584	−0.330	−0.760	0.372	−0.321	0.190
2	0	−9.486		−9.372		−9.503	0.255		
2	1	0.176	0.444	0.161	0.440	0.145	0.196	0.484	0.128
2	2	13.660	6.603	13.472	6.538	13.665	0.451	0.676	0.353
3	0	0.923		0.912		0.884	0.177		
3	1	0.745	−0.438	0.679	−0.431	0.769	0.362	−0.437	0.128
3	2	−1.581	−0.585	−1.557	−0.583	−1.577	0.228	−0.534	0.104
3	3	−3.452	1.443	−3.318	1.438	−3.527	0.481	1.420	0.312
4	0	4.998		4.845		4.958	0.314		
4	1	−0.767	−0.341	−0.737	−0.338	−0.725	0.275	−0.389	0.116
4	2	−6.895	−2.607	−6.682	−2.540	−6.836	0.415	−2.625	0.266
4	3	0.646	0.585	0.620	0.579	0.532	0.224	0.599	0.194
4	4	6.853	5.466	6.621	5.324	6.735	0.598	5.493	0.454
5	0	−0.617		−0.593		−0.520	0.295		
5	1	−1.384	0.441	−1.246	0.439	−1.407	0.665	0.455	0.143
5	2	1.157	0.263	1.113	0.268	1.084	0.335	0.245	0.168
5	3	2.916	−0.689	2.725	−0.699	3.007	0.660	−0.691	0.389
5	4	−1.466	−0.956	−1.408	−0.948	−1.482	0.252	−1.027	0.223
5	5	−6.908	−0.294	−6.563	−0.204	−7.109	0.961	−0.425	0.564
6	0	−4.952		−4.690		−4.925	0.662		
6	1	1.128	0.119	1.051	0.115	0.957	0.645	0.132	0.148
6	2	6.540	2.062	6.189	1.958	6.456	0.884	2.085	0.352
6	3	−0.952	−0.348	−0.885	−0.339	−0.706	0.560	−0.348	0.296
6	4	−5.529	−3.745	−5.216	−3.558	−5.390	0.905	−3.741	0.518
6	5	0.961	0.579	0.893	0.576	0.698	0.459	0.499	0.320
6	6	6.269	5.480	5.901	5.203	6.143	1.298	5.427	0.793
7	0	0.979		0.913		0.806	0.709		
7	1	2.871	−0.333	2.565	−0.343	2.993	1.431	−0.367	0.205
7	2	−1.639	−0.053	−1.530	−0.058	−1.476	0.934	−0.004	0.278
7	3	−4.202	0.551	−3.839	0.600	−4.429	1.422	0.568	0.544
7	4	1.931	0.687	1.799	0.671	1.855	0.839	0.767	0.362
7	5	6.648	0.694	6.176	0.536	6.916	1.532	0.866	0.773
7	6	−1.813	−1.574	−1.675	−1.524	−1.732	0.800	−1.798	0.356
7	7	−11.486	−5.244	−10.781	−4.784	−11.831	2.164	−5.702	1.413
8	0	6.512		6.033		6.585	1.497		
8	1	−2.304	−0.200	−2.124	−0.182	−1.967	1.673	−0.213	0.258
8	2	−8.618	−2.495	−7.975	−2.311	−8.628	2.035	−2.603	0.656
8	3	2.054	0.474	1.885	0.435	1.583	1.610	0.442	0.583
8	4	7.262	4.213	6.699	3.885	7.121	2.030	4.252	1.022
8	5	−1.818	−0.585	−1.645	−0.553	−1.259	1.451	−0.397	0.739
8	6	−6.545	−5.041	−6.028	−6.623	−6.472	2.219	−4.879	1.266
8	7	1.989	0.896	1.767	0.871	1.533	1.117	0.566	0.853
8	8	9.895	7.341	9.161	6.742	10.190	3.255	7.363	1.975
9	0	−2.134		−2.001		−1.853	2.085		
9	1	−5.404	0.278	−4.754	0.318	−5.760	3.302	0.357	0.381
9	2	3.284	0.118	3.068	0.101	2.999	2.842	0.014	0.583
9	3	6.973	−0.243	6.262	−0.387	7.554	3.284	−0.309	1.038
9	4	−3.613	−0.809	−3.347	−0.743	−3.465	2.659	−0.834	0.879
9	5	−9.483	−1.500	−8.673	−1.166	−10.216	3.392	−1.746	1.553
9	6	3.362	1.901	3.059	1.770	3.107	2.488	2.113	0.931
9	7	12.075	5.737	11.166	5.077	12.739	3.696	6.422	2.223
9	8	−2.416	−2.810	−2.114	−2.643	−1.918	2.339	−3.107	0.948
9	9	−16.368	−15.465	−15.252	−14.149	−17.161	4.819	−16.809	4.147

Numbers in brackets denote the shifts determined through estimation of generalized moments of inertia as given in Table I.

Acknowledgements

This work was supported by the KBN Grant 2 2104 9203 and by the NCU Grant 682-A. The first author wishes to express his gratitude to prof. Drożyner for the opportunity to use the SUN-10 system (KBN Grant) for calculations.

References

Antonov, W. A., Timoshkova, E. I., Holshevnikov, K. W.: 1988, *Introduction to the Theory of the Newtonian Potential*, Moscow, Nauka, pp. 133–147, (in Russian).

Bevington, P. R.: 1969, *Data Reduction and Error Analysis for Physical Sciences*, McGraw-Hill Book Comp., New York.

Bills, B. G. and Ferrari, A. J.: 1978, 'Mars Topography Harmonics and Geophysical Implications', *J. Geophys. Res.* **83**, 3497–3508.

Chao, B. F. and Rubincam, D. P.: 1989, 'The Gravitational Field of Phobos', *Geoph. Res. Lett.* **16**, 859–862.

Duboshin, G. H.: 1975, *Celestial Mechanics: Basic Problems and Methods*, Nauka, Moscow.

Duxbury, T. C.: 1989, The Figure of Phobos, *Icarus*, **78**, 169–180.

Edmonds, A. R.: 1957, *Angular Momentum in Quantum Mechanics*, Princeton Univ. Press.

Martineč, Z., Pěč, K. and Burša, M.: 1989, 'The Phobos Gravitational Field Modeled on the Basis of its Topography', *Earth, Moon and Planets*, **45**, 219–235.

Landau, L. D. and Lifshyc, E. M.: 1974, *The Quantum Mechanics, Nonrelativistic Theory*, Nauka, Moscow (in Russian).

Pěč, K., Marinec, Z.: 1983, 'Expansion of the of the Geoid Heights Over a Triaxial Earth's Ellipsoid into a Spherical Harmonic Series', *Studia Geoph. et Geod.* **27**, 227–230.

Paul, M. K.: 1988, 'An Expansion in Power Series of Mutual Potential for Gravitating Bodies with Finite Sizes', *Celest. Mech.* **44**, 49–59.

Press, W. H., Teukolsky, S. A., Vetterling, W. T., and Flannery, B. P.: 1992, *Numerical Recipes in FORTRAN, The Art of Scientific Computing*, Second Edition, Cambridge Univ. Press.

Sagitov, M. U., Tadzhidinov, Kh. G. and Mikhailov, B. O.: 1981, 'On the Phobos Gravitational Field Model', *Astron. Vest.* **XV**, No. 3, 142–152.

Šlidl'ichovsky, M.: 1978, 'The Force Function of two General Bodies', *Bull. Astron. Inst. Czechosl.* **29**, 90–97.

Stooke, P. J.: 1992, 'A Model and Map of Amalthea', *Earth, Moon and Planets*, **56**, 123–139.

Stooke, P. J.: 1994, 'The Geology of Amalthea', *Earth, Moon and Planets*, in press.

Veverka, J., Thomas, P., Davies, M. and Morrison, D.: 1981, 'Amalthea: Voyager Imaging Results', *J. Geoph. Res.* **86**, 8675–8692.